

DEVICE DISPERSION AND INTERMODULATION IN HEMTs

James Brinkhoff and Anthony E. Parker

*Department of Electronics, Macquarie University, Sydney AUSTRALIA 2109,
mailto: jamesb@ics.mq.edu.au*

ABSTRACT

It has been shown previously that bias networks in microwave amplifiers can lead to complex intermodulation distortion effects. Here, we demonstrate that charge trapping effects in High Electron Mobility Transistors (HEMTs) can lead to additional anomalous intermodulation behaviour. This behaviour can be clearly observed as changes in intermodulation levels with tone-spacing, and two-tone asymmetry. Simulations using a simple model, that includes hole trapping effects, predicts similar intermodulation behaviour to measured behaviour. A Volterra-series analysis allows an understanding of the mechanisms involved.

INTRODUCTION

Memory effects have been identified as a major obstacle in designing highly linear amplifiers for wireless systems [1]. Memory in this context can be defined as a variation of amplifier distortion characteristics with signal bandwidth. These effects can cause intermodulation levels to vary with signal bandwidth, and asymmetry between upper and lower intermodulation levels.

These often observed effects lead to difficulty in finding linearity specifications of amplifiers. If the two intermodulation levels are different, which one should be used? If the intermodulation levels change with different tone-spacings, which tone-spacing should be selected? They also lead to difficulty in predicting and reducing distortion. Common linearization techniques are rendered ineffective because they rely on constant and equal intermodulation levels over the signal bandwidth [1]. Thus, it is important to understand these effects, in order to be able to reduce or compensate for them.

A number of works have clearly demonstrated the link between changing second-order impedances (such as bias networks and second-harmonic terminations) and memory effects [2]. In addition, low frequency thermal variations of active devices have been shown to cause memory effects [3].

Some authors have postulated that semiconductor charge trapping mechanisms could be another source of memory [3]. These effects cause a variation in the low frequency characteristics of circuits (variation in HEMT drain conductance and transconductance), just as bias networks and thermal variations do [4]. However, a demonstration of this link between trapping and memory effects has not been made.

This paper aims to provide a demonstration that trapping effects can influence intermodulation, through measurement and simulation. Only hole trapping is considered, because this is believed to be the dominant cause of memory effects in the HEMT measurements reported in this paper. The power levels are set to ensure weakly nonlinear behaviour, so that truncated Taylor-series can be used to model the nonlinearities.

The next section reviews the theory on how bias networks can affect intermodulation. Then, measurements of a HEMT that shows evidence of trapping influencing intermodulation are discussed. It is shown that a simple HEMT model (that includes hole trapping due to impact ionization) can predict similar intermodulation behaviour to that measured. A Volterra-series analysis of a HEMT with hole traps is derived, allowing an analytic understanding of the underlying mechanisms responsible for intermodulation dependence on trapping.

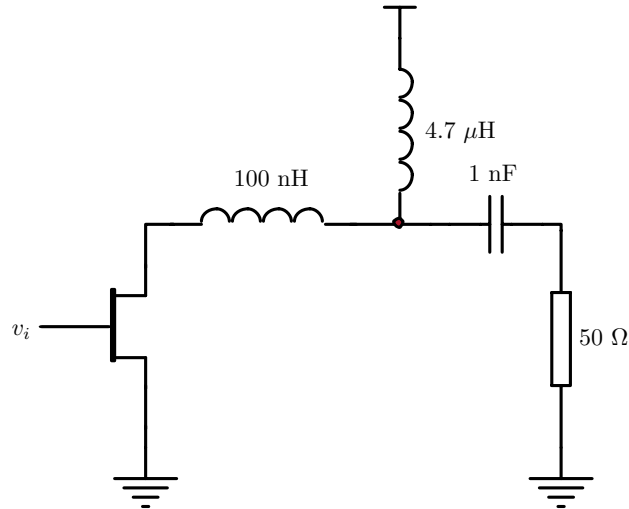


Fig. 1. Simple HEMT amplifier circuit, indicating drain load, bias network, and matching network.

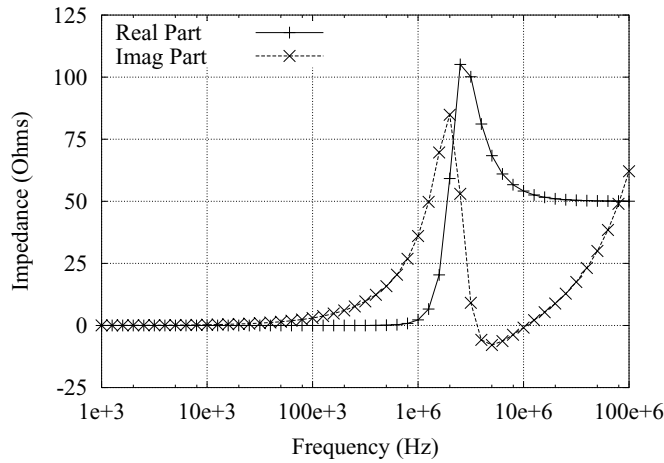


Fig. 2. Typical impedance presented to the drain of a HEMT, due to the combined load, bias network and matching network.

BIAS NETWORK EFFECTS

A number of authors have demonstrated that bias networks can be a major source of memory effects in microwave amplifier circuits. Even if the centre frequency of the signal being amplified is much higher than the resonant frequency of the bias network, these effects still occur. To explain how this occurs, a simple HEMT amplifier is considered as shown in Fig. 1.

Fig. 2 shows the impedance presented to the drain of the HEMT in Fig. 1 due to the load, bias network and matching network. At very low frequencies, the impedance is near a short due to the RF choke. At high frequencies, the impedance becomes the load transformed by the matching network. In between these frequency extremes, there are large changes in the drain impedance.

A previously published Volterra-series analysis [5] has been shown to accurately predict measured intermodulation levels at low frequencies. If $v_i = 2V_s \cos(\omega_c t) \cos(\frac{\Delta\omega}{2} t)$ (a two-tone input signal), one of the intermodulation levels will be:

$$V_{o3} = V_s^3 Z_o(\omega_c) \left(c_1 + c_2 Z_o(2\omega_c) + c_0 Z_o(\Delta\omega) \right) \quad (1)$$

In this equation, $Z_o(\omega)$ is the frequency dependent drain impedance in parallel with the drain conductance. The coefficients c_0 , c_1 and c_2 are dependent on bias (because they include terms in a Taylor-series expansion of the

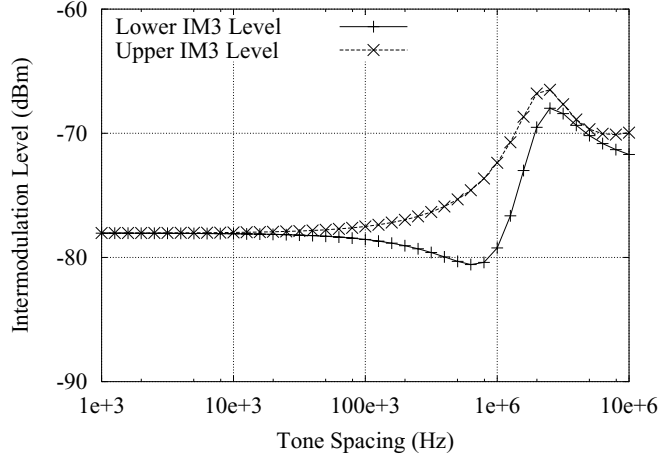


Fig. 3. Simulated intermodulation levels with varying tone spacing for the circuit in Fig. 1. The input tones were at -21 dBm, and the lower tone is 50 MHz.

nonlinear drain current) and carrier frequency. They are reproduced in the appendix.

It can be seen from (1), that the intermodulation levels are not only dependent on the drain impedance near the carrier frequency. They also depend on the drain impedance at the second-harmonic and difference (or envelope) frequencies. Therefore, if the drain impedance is changing over the range of modulation frequencies in a complex signal, or over the range of tone-spacings used in intermodulation tests, then the intermodulation levels can change.

Intermodulation levels with varying tone spacing for the circuit in Fig. 1 are shown in Fig. 3. The HEMT model used is given later. It can be seen that the intermodulation levels change over the range of tone spacings where the bias network impedance changes, Fig. 2. Also, there is asymmetry between the upper and low intermodulation tones at some tone spacings. These effects are due to the term $c_0 Z_o(\Delta\omega)$ in (1). The coefficient c_0 is defined in the Appendix, and $Z_o(\Delta\omega)$ is the effective drain impedance at baseband frequencies (typically determined by the bias network). It was shown in [5] that there are biases where c_0 is close to zero, and therefore these memory effects due to bias networks become negligible.

It is sometimes possible to design the bias networks so that their impedance does not change over the range of frequencies that may be present in the modulating signal. This is especially true in narrow-band amplifier designs, where $\omega_c \gg \Delta\omega$. However, memory effects are sometimes still observed, especially in highly linear amplifiers. These must be due to effects within the device itself, such as thermal variations or charge trapping.

HEMT MEASUREMENTS

Intermodulation measurements were performed on a number of HEMTs. They were biased near the intermodulation null [6] so that any variation in intermodulation would be very noticeable. The measurements presented here were for a GaAs HEMT with pinch-off voltage of -1 V, and a gate width of 120 μm . The input power was -21 dBm per tone, ensuring weakly nonlinear operation. The lower tone was 4 GHz, and the upper tone was swept from 4 GHz+1 kHz to 5 GHz.

The measured intermodulation levels at drain biases of 3.5 V and 3.7 V are shown in Fig. 4. Above tone-spacings of 10 MHz, there are changes in the intermodulation levels, which are due to the changing bias network impedances at these frequencies. The 'jumps' in the intermodulation levels at these high tone spacings are probably due to the rapidly changing impedance presented to the drain of the device, because the interconnect from the bias tee to the on-wafer device is electrically long.

There are also significant changes in the intermodulation levels at tone-spacings less than 10 MHz. These cannot be due to the bias networks, since the bias network impedance is constant at those frequencies. There are large asymmetries in the intermodulation levels at tone-spacings near 100 kHz. Also notice that the tone-spacing where the large dip in the lower intermodulation occurs increases with drain bias. This dependency has been observed in

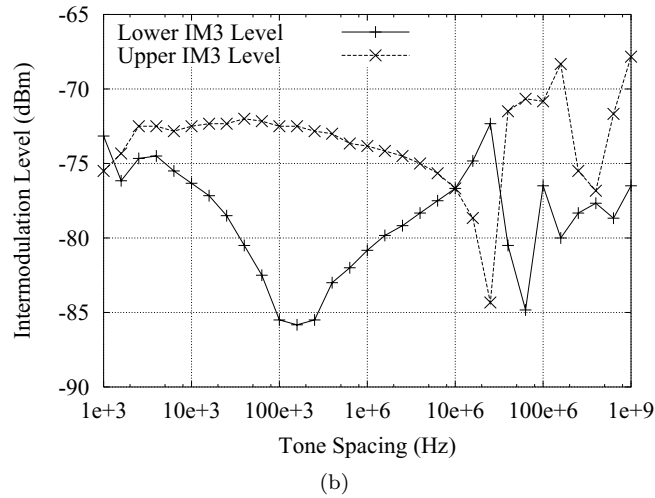
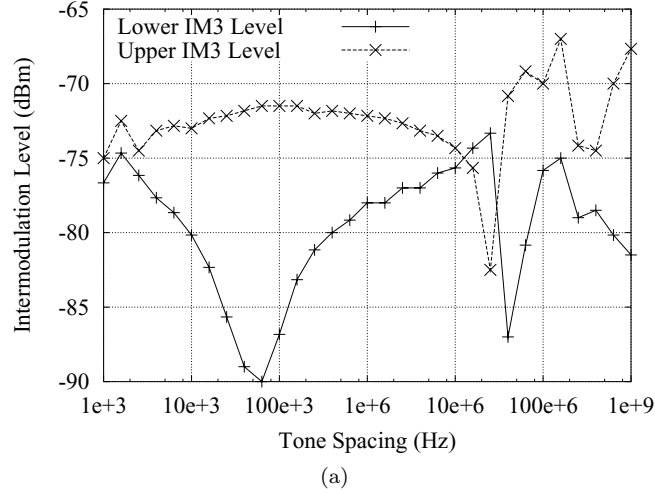


Fig. 4. Measured intermodulation levels vs tone spacing of a GaAs HEMT for two drain biases. The gate bias was -0.92 V, the lower tone was 4 GHz, and the input power was -21 dBm. (a) Drain bias at 3.5 V. (b) Drain bias at 3.7 V.

different HEMT devices, and over a wide range of drain biases.

It seems likely that these effects are due to charge trapping mechanisms in the device. The dispersion of the drain conductance over frequency was measured with a low-frequency network analyser. This measurement has often been used to identify trapping effects [4]. The real and imaginary parts of the drain conductance of the HEMT are shown in Fig. 5. These measurements show evidence of dispersion due to hole trapping. These evidences are (see [4]):

- The drain conductance reduces with increasing frequency.
- The onset of this negative dispersion begins at a certain drain voltage (~ 3 V in this case).
- The frequency at which the drain conductance changes increases with drain bias. This is linked with the increase in the frequency of the dip in intermodulation with drain bias (Fig. 4).

It is also important to note that at the frequencies at which the drain conductance is changing, there is a significant imaginary component (or phase shift) in the drain conductance. It will be shown in the next section that this imaginary part can lead to the large asymmetry that is observed between the intermodulation levels.

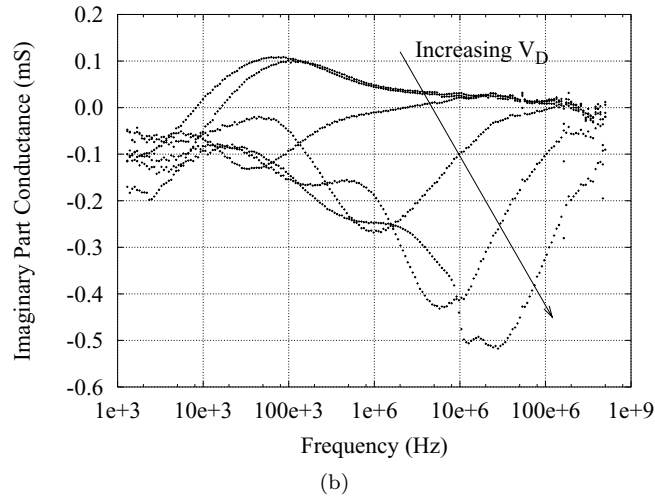
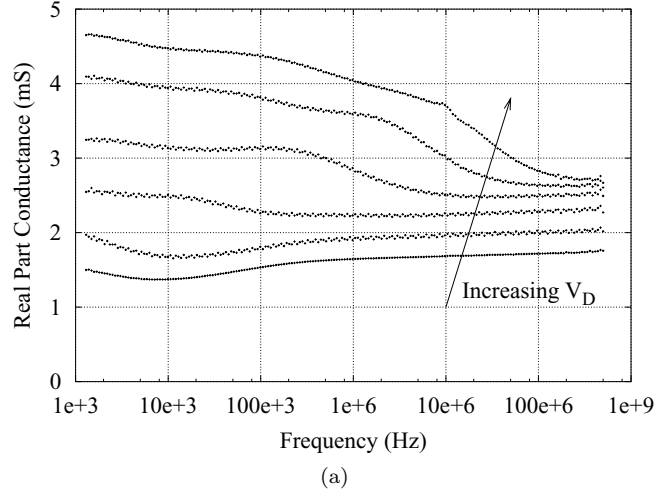


Fig. 5. Measured drain conductance variation with frequency for the GaAs HEMT with a gate bias of -0.9 V and drain bias from 2 V to 4.5 V in steps of 0.5 V. (a) Real part of drain conductance. (b) Imaginary part of drain conductance.

MODEL

A demonstrative model was used in [4] to explain the dispersion in transconductance and drain conductance, which is due to electron and hole trapping phenomena, as well as thermal variation. This model was able to produce the main features of the dispersive low frequency gain of a typical HEMT. Impact ionization, which leads to the trapping of holes near the gate region, is often present in HEMT devices. Thus, in this paper, we consider only the hole trapping dispersion mechanism, which is sufficient to explain the dominant features of the intermodulation effects in the HEMTs we measured. It should be emphasised that this simple model is not intended to predict the measured distortion. Rather, it is used to form the basis for an understanding of how trapping affects intermodulation, which should enable the development of an accurate model in the future.

As the drain voltage increases, impact ionization begins to occur, causing holes to travel back through the device towards the source. Some of these holes are trapped and released at slow rates, which causes a variation in the threshold voltage of the device at low frequencies. The drain current model including hole trapping, which is explained in [4], is

$$i_{DS} = \beta(v_{GS} + \gamma v_{DS} + \overline{v_H} - V_T)^2 \tanh(\alpha v_{DS}) \quad (2)$$

The slow varying potential $\overline{v_H}$ is the effective hole trap potential, and is given by the following differential equation:

$$V_H \ln(f_{II} + 1) = \overline{v_H} + \frac{\tau}{f_{II}} \frac{d}{dt} \overline{v_H} \quad (3)$$

$$f_{II} = \exp\left(\frac{-B}{v_{DS} - V_S + \sqrt{(v_{DS} - V_S)^2 + 2}}\right) \quad (4)$$

It is possible to enter this model into a transient or harmonic-balance simulator and observe the effects of altering device parameters on intermodulation performance. However, this does not provide an analytic understanding of how the device characteristics are affecting the intermodulation. A powerful analytic tool, called Volterra-series analysis [7] can be used to find closed-form expressions for the distortion products. This is the method used to produce the results below.

The drain current is represented by a 2-Dimensional Taylor-series expansion around the bias point, up to the third order:

$$i_d = G_m v_g + G_d v_d + G_{m2} v_g^2 + G_{md} v_g v_d + G_{d2} v_d^2 + G_{m3} v_g^3 + G_{m2d} v_g^2 v_d + G_{md2} v_g v_d^2 + G_{d3} v_d^3 \quad (5)$$

The effective hole trap potential (3) is a nonlinear function of the drain voltage. This voltage then, can be represented by a second-order Taylor-series with respect to drain voltage, filtered by some low-pass function $F(\omega)$. Terms above second-order are not considered, as only terms that are in the passband of the low-pass function $F(\omega)$ are important. Thus, the hole trap potential is represented by:

$$\overline{v_h}(\omega) = F(\omega)(v_d + G_{h2} v_d^2) \quad (6)$$

The gate voltage is then given by $v_g = v_i - \overline{v_h}$. The goal of our analysis is to find the relationship between the two-tone input signal v_i , and the distorted output signal v_o .

First, the linear response is considered. If $v_i = V_s \cos(\omega_1 t)$ then the magnitude of the output voltage at that frequency is

$$V_{o1}(\omega_1) = V_s A(\omega_1) \quad (7)$$

where the gain is

$$A(\omega) = -G_m \frac{Z_d(\omega)}{1 + Z_d(\omega)(G_d + G_m F(\omega))} \quad (8)$$

This predicts that at low frequencies when $F(\omega)$ is significant, the hole traps cause dispersion in the gain and drain conductance, as observed in Fig. 5. The effective drain conductance varies with frequency, and is given by:

$$G_{def}(\omega) = G_d + G_m F(\omega) \quad (9)$$

Then, the second- and third-order nonlinear transfer function are found using the method in [7]. These results are then simplified algebraically. It is assumed that the trapping effect has negligible impact at the carrier frequency. The effective drain termination (drain impedance in parallel with HEMT output conductance) is

$$Z_o(\omega) = \frac{Z_d(\omega)}{1 + Z_d(\omega)G_d} \quad (10)$$

A two tone input signal $v_i = V_s (\cos(\omega_1 t) + \cos(\omega_2 t))$ is applied, with $\omega_1 \approx \omega_2 \approx \omega_c$, and $\omega_2 - \omega_1 = \Delta\omega$. Then, the upper and low intermodulation products are:

$$V_{o3}(2\omega_1 - \omega_2) = V_s^3 Z_o(\omega_c) \left(c_1 + c_2 Z_o(2\omega_c) + c_0 Z_o(-\Delta\omega) + c_h F(-\Delta\omega) \right) \quad (11)$$

$$V_{o3}(2\omega_2 - \omega_1) = V_s^3 Z_o(\omega_c) \left(c_1 + c_2 Z_o(2\omega_c) + c_0 Z_o(\Delta\omega) + c_h F(\Delta\omega) \right) \quad (12)$$

Equations (11) and (12) have been arranged to show the intermodulation dependence on impedance $Z_o(\omega)$ and the trap low-pass function $F(\omega)$ at the various frequencies. If $F(\omega)$ is made zero, so that there are no trapping effects,

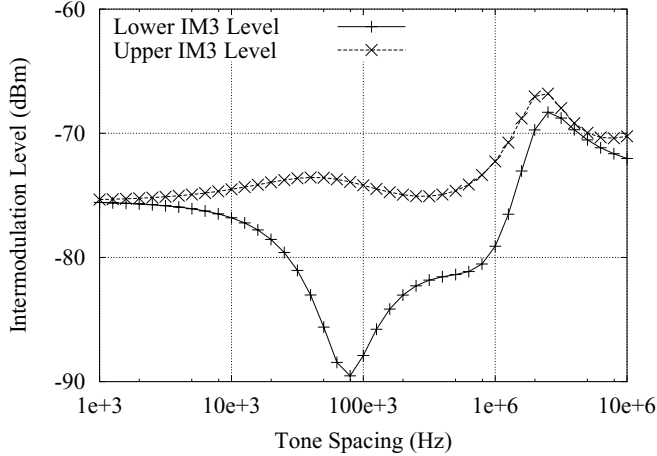


Fig. 6. Simulated intermodulation levels with varying tone spacing using the equation in (11) and (12). The drain bias is 3.5 V and the gate bias is -0.9 V. The input tones were at -21 dBm, and the lower tone is 50 MHz. The model parameters are: $\beta = 0.05 \text{ A}\cdot\text{V}^{-2}$, $\gamma = 0.06$, $V_T = -1 \text{ V}$, $\alpha = 4 \text{ V}^{-1}$, $V_H = 0.2 \text{ V}$, $\tau = 400 \text{ ns}$, $B = 2 \text{ V}$, and $V_S = 4 \text{ V}$. The drain network is as shown in Fig. 1.

the model reduces to that presented in [5], which has been shown to predict intermodulation and its dependence on baseband impedance well, when other memory effects are not significant. Each of the coefficients c_1 , c_2 , c_0 and c_h are bias dependent, and depend only on impedances and nonlinearities at the fundamental frequencies. They are given in the appendix for interested readers.

This model was used to simulate the intermodulation levels. The Taylor-series coefficients of drain current in (5) and of trap potential in (6) were calculated from the model current equation (2) in a mathematical software package. The simulated levels using the Volterra model presented above are shown in Fig. 6. The simulation shows a similar behaviour to the measured behaviour, in that there is variation in intermodulation due to the bias network at large tone spacing ($>1 \text{ MHz}$). Note that the bias network used in the simulation is much simpler than the one used for the measurements in Fig. 4. There is the large dip in the lower intermodulation level, which is due to the hole trapping, and predicted by the term $c_h F(-\Delta\omega)$ in (11). In addition, the frequency at which this dip occurs in the simulation, increases as the drain bias increases, as was observed in the measurements, Fig. 4. This further increases confidence that charge trapping effects can be responsible for intermodulation memory effects.

The equations (11) and (12) provide a useful means to understanding the mechanisms that cause semiconductor trapping to affect intermodulation levels. The baseband and second-harmonic impedance dependency of intermodulation ($c_2 Z_o(2\omega_c) + c_0 Z_o(\Delta\omega)$) has already been explained in [5]. The effects of hole trapping on intermodulation can be explained as follows. The drain voltage components at the two fundamental frequencies are mixed by the second-order nonlinearity, g_{h2} , in the trapping mechanism, giving a component of the trap voltage, v_h , at $\Delta\omega$. This is then mixed up to an intermodulation frequency by second-order device nonlinearity. The hole trapping effect is accounted for in the term $c_h F(\Delta\omega)$ in (11).

This extra term caused by hole trapping can have two easily observable effects on intermodulation in a two-tone test. They can cause the intermodulation levels to change as the tone spacing changes, and they can cause asymmetry. The change in intermodulation comes about simply because $F(\Delta\omega)$ varies with the tone spacing $\Delta\omega$, (as measured in the dispersion of the drain conductance). Asymmetry can occur if the imaginary components in the terms dependent on $F(\omega)$ add and subtract from the imaginary components in the other terms, see (11) and (12). A vector diagram of this is shown in Fig. 7. Thus, because trapping effects cause the output conductance to be complex, intermodulation level asymmetry can occur even if there is zero baseband impedance.

CONCLUSION

The effects of bias networks on intermodulation have been reviewed. HEMT measurements with intermodulation level changes and asymmetries (memory effects) that could not be explained by bias network effects were discussed.

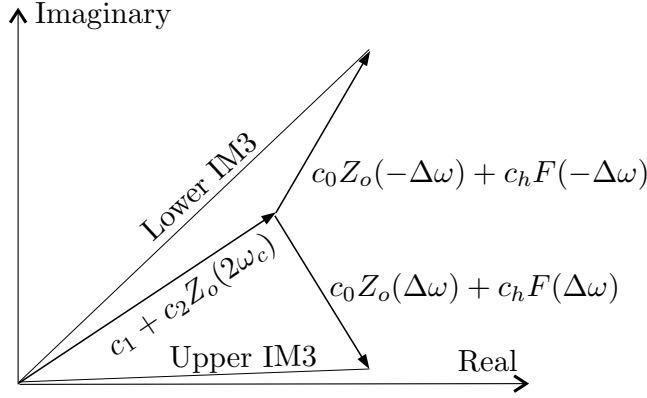


Fig. 7. Vector diagram showing how asymmetry in intermodulation levels can occur. The upper and lower intermodulation levels have $c_1 + c_2 Z_o(2\omega_c)$ in common. The upper intermodulation level adds $c_0 Z_o(\Delta\omega) + c_h F(\Delta\omega)$, while the lower level adds its complex conjugate $c_0 Z_o(-\Delta\omega) + c_h F(-\Delta\omega)$, leading to the possibility of unequal intermodulation products if these terms are complex.

We showed that these memory effects are most probably due to hole trapping effects, because of their bias dependent frequency dispersion, their bias dependent change in the frequency of the intermodulation dip, and because similar effects were predicted by a simple model of a HEMT with hole trapping. A Volterra-series analysis of the HEMT allowed an understanding of how the effects arise. This will allow methods to be developed to predict and reduce these effects, so that more accurate models and more linear amplifiers can be designed.

ACKNOWLEDGEMENTS

The authors thank the Commonwealth Scientific and Industrial Research Organization (CSIRO) Telecommunications and Industrial Physics, Sydney, N.S.W., Australia, and Dr. J. W. Archer, CSIRO, for their support.

References

- [1] J. Vuolevi, J. Manninen, and T. Rahkonen, "Cancelling the memory effects in RF power amplifiers," in *IEEE Int. Symp. Circuits and Systems*, pp. 57–60, 2001.
- [2] N. B. de Carvalho and J. C. Pedro, "Two-tone IMD asymmetry in microwave power amplifiers," in *IEEE MTT-S Int. Microwave Symp. Dig.*, vol. 1, (Boston, MA), pp. 445–448, 2000.
- [3] N. L. Gallou, J. M. Nebus, E. Ngoya, and H. Buret, "Analysis of low frequency memory and influence on solid state HPA intermodulation characteristics," in *IEEE MTT-S Int. Microwave Symp. Dig.*, pp. 979–982, 2001.
- [4] A. E. Parker and J. G. Rathmell, "Bias and frequency dependence of FET characteristics," *IEEE Trans. Microwave Theory Tech.*, vol. 51, pp. 588–592, February 2003.
- [5] J. Brinkhoff and A. E. Parker, "Effect of baseband impedance on FET intermodulation," *IEEE Trans. Microwave Theory Tech.*, vol. 51, pp. 1045–1051, March 2003.
- [6] A. E. Parker and G. Qu, "Intermodulation nulling in HEMT common source amplifiers," *IEEE Microwave and Guided Wave Letters*, vol. 11, pp. 109–111, March 2001.
- [7] S. A. Maas, *Nonlinear Microwave Circuits*. Norwood, MA: Artech House, 1988.

APPENDIX

$$\begin{aligned}
 c_0 &= \frac{1}{2} \left(G_{m2} + \frac{1}{2} G_{md} (A(\omega_c) + A(-\omega_c)) + G_{d2} A(\omega_c) A(-\omega_c) \right) (G_{md} + 2G_{d2} A(\omega_c)) \\
 c_1 &= -\frac{3}{4} \left(G_{m3} + \frac{1}{3} G_{m2d} (2A(\omega_c) + A(-\omega_c)) + \frac{1}{3} G_{md2} (2A(\omega_c) A(-\omega_c) + A(\omega_c)^2) + G_{d3} A(\omega_c)^2 A(-\omega_c) \right) \\
 c_2 &= \frac{1}{4} \left(G_{m2} + G_{md} A(\omega_c) + G_{d2} A(\omega_c)^2 \right) (G_{md} + 2G_{d2} A(-\omega_c)) \\
 c_h &= -\frac{1}{2} (2G_{m2} + G_{md} A(\omega_c)) (G_{h2} A(\omega_c) A(-\omega_c))
 \end{aligned}$$